THE JOURNAL OF PHYSICAL CHEMISTRY C

Article

Calculated Thermal Properties of Single-Walled Carbon Nanotube Suspensions

Hai M. Duong, Dimitrios V. Papavassiliou, Kieran J. Mullen, Brian L. Wardle, and Shigeo Maruyama

J. Phys. Chem. C, **2008**, 112 (50), 19860-19865 • Publication Date (Web): 21 November 2008

Calculated Thermal Properties of Single-Walled Carbon Nanotube Suspensions

Hai M. Duong,[†] Dimitrios V. Papavassiliou,*[,‡] Kieran J. Mullen,[§] Brian L. Wardle,[||] and Shigeo Maruyama[†]

Department of Mechanical Engineering, The University of Tokyo, Tokyo 113-8656, Japan, School of Chemical, Biological and Materials Engineering, and The Homer L. Dodge Department of Physics and Astronomy, The University of Oklahoma, Norman, Oklahoma 73019-0390, and Department of Aeronautics and Astronautics, Massachusetts Institute of Technology, Cambridge, Massachusetts 02139-4307

Received: October 15, 2007; Revised Manuscript Received: June 2, 2008

The present work is a systematic numerical study of the thermal properties of single-walled carbon nanotubes (SWNTs) in suspensions. A computational model, based on the simulation of the random movement of Brownian thermal walkers in aqueous and in oil suspensions of SWNTs, was used to investigate the effect of the SWNT aspect ratio, weight fraction, and interfacial thermal resistance on effective thermal properties of the suspension. The dependence of the effective thermal conductivity on the temperature for aqueous suspensions was also investigated.

1. Introduction

Recent studies show that the incorporation of single-walled carbon nanotubes (SWNTs) could enhance mechanical and electrical transport properties[1] and thermal transport properties[2,3] of materials. Few investigations have focused on the thermal conductivity of fluids containing dispersed SWNTs. Traditional models of the effective thermal conductivity of suspensions are based on microscopic rather than nanoscale considerations. They have been derived assuming that the continuum approximation holds, and they do not account for ballistic heat transfer. The variables that determine the effective conductivity in traditional models are the particle shape and the volume fraction.[4,5] However, the thermal conductivity of nanofluids also depends on possible epitaxial layering of the fluid molecules in the molecular layers adjacent to the suspended nanoparticles[6] and on the temperature. The existence of a thermal resistance[7−11] to the transfer of heat between the nanoscale inclusions (SWNTs) and the surrounding matrix (suspending liquid) can also result in anomalous heat transfer behavior. As there are no accurate and reliable theoretical formulas currently available to predict the thermal conductivity of nanofluids satisfactorily, it is important to systematically explore the thermal properties of SWNT-in-fluid suspensions by a numerical method.

Previous studies of the thermal conductivity of SWNT suspensions and the thermal resistance of the SWNT−matrix interface include the work of Maruyama et al.,[10] who studied the thermal conductance between a SWNT and confined water by molecular dynamics (MD) simulations. A (10, 10) SWNT with a length of 20.1 nm and a diameter of approximately 1.0 nm was simulated in a 20.1 × 10 × 10 nm fully periodic simulation cell. The SWNT contained 192 water molecules in its hollow space. Initially, water molecules and the SWNT were equilibrated at 300 °C, and then the SWNT was suddenly heated to 400 °C. By observing the heat transfer from the heated SWNT to the water, and using the lumped capacity method, Maruyama et al.[10] found that the thermal boundary resistance R_{bd} between the SWNT and the water was 2.0×10^{-7} m^2·K/W (thermal boundary conductance, $K_{bd} = 1/R_{bd} = 5$ MW/m^2·K). Huxtable et al.[11] used picosecond transient adsorption to measure the interface thermal conductance of carbon nanotubes suspended in surfactant micelles in water. Their experimental results showed that the interface thermal conductance did not depend critically on the surfactant as long as the surfactant was not covalently bonded to the nanotube. The thermal boundary resistance was measured to be 0.83×10^{-7} m^2·K/W ($K_{bd} = 12$ MW/m^2·K). Huxtable et al.[11] also conducted MD simulations of heat flow from (5,5) SWNTs of various lengths to a surrounding octane liquid kept at standard conditions. Through the equilibration simulations, the thermal boundary resistance between the SWNTs and octane was calculated to be 0.4×10^{-7} m^2·K/W ($K_{bd} = 25$ MW/m^2·K). Even though both MD and experimental results are very rough estimates, one could assume that the typical thermal boundary resistance between SWNTs and such fluids is in the range of $(0.4-2.0) \times 10^{-7}$ m^2·K/W ($K_{bd} = 5-25$ MW/m^2·K).

The simulation and experimental data reviewed above were used to study the thermal conductivities of SWNTs in water and engine oil suspensions in the present work. Table 1 shows the technical data of engine oil and water at different temperatures, and the velocity of sound used for the simulations. The thermal conductivity of SWNTs dispersed randomly in water and engine oil and its temperature dependence were studied by the random walk algorithm of Duong et al.[12] This computational model is an improvement of previous Monte Carlo-based models[13−15] and has been validated with experimental data on SWNT−polymer composites.[12] The random walk algorithm is much faster than an MD algorithm. Because the carbon nanotube thermal conductivity is several orders of magnitude larger than the thermal conductivity of the fluid surrounding the SWNTs, there is no need to model random walks within the nanotubes. One can instead assume a uniform distribution of thermal walkers inside each SWNT, which is equivalent to assuming a

* Corresponding author. Tel./fax: (405) 325-5811/(405) 325-5813. E-mail: dvpapava@ou.edu.
[†] Department of Mechanical Engineering, The University of Tokyo.
[‡] School of Chemical, Biological and Materials Engineering, The University of Oklahoma.
[§] The Homer L. Dodge Department of Physics and Astronomy, The University of Oklahoma.
[||] Department of Aeronautics and Astronautics, Massachusetts Institute of Technology.

10.1021/jp710021n CCC: $40.75
Published on Web 11/21/2008

TABLE 1: Properties of Oil and Water Used in the Simulations

suspensions	oil at 40 °C[a]	water at 20 °C[b]	water at 40 °C[b]	water at 60 °C[b]	water at 80 °C[b]
density, g/cm^3	0.819	0.998	0.992	0.983	0.972
specific heat capacity, J/g·K	2.222	4.182	4.178	4.184	4.196
thermal conductivity, W/mK	0.145	0.598	0.630	0.654	0.670
thermal diffusivity, nm^2/ns	79.67	143.35	152.07	159.04	164.29
velocity of sound, m/s[c]	1477.00	1496.70	1496.70	1496.70	1496.70

[a] Glavatskih et al.[24] [b] *Handbook of Chemistry and Physics*, pp 6-9 and 6-10.[25] [c] Velocity of sound is obtained from *Handbook of Chemistry and Physics, Velocity of Sound in Various Media*, pp 14−35. Water and oil are considered as distilled water and castor oil, respectively.[26]

thermal conductivity for the SWNTs that tends to become infinite when compared to the conductivity of the fluid.

The effects of different weight fractions and aspect ratios of SWNTs in the suspension and of different thermal boundary resistance on the suspension effective properties are quantified in this work. As there has been no experimental or simulation work studying the temperature dependence of the effective thermal conductivity of the SWNT suspensions, the thermal conductivity dependence on temperature of the SWNT-in-water suspension is also studied. Liquid suspension of SWNTs is a basic step in the separation process of nanotube bundles, or of sorting nanotubes by length, diameter, or roll-up vector, and is important in the processing of composites in liquid polymer matrices.[16,17] Understanding the thermal properties of SWNT suspensions can be important in scaling up and optimizing such processes.

2. Simulation Methodology

The aspect ratio of SWNTs, as found from experiments, is very large, because the average SWNT diameter, D, is usually not greater than 3.0 nm, while the length of SWNTs, L, can be up to several micrometers.[18] Molecular dynamics[19] simulations predicted length dependence of the thermal conductivity of SWNTs, and recent measurements by Wang et al.[20] have shown that the thermal conductivity of SWNTs depends on their length for $L < 2.5$ μm. However, the measured change was from ~2600 W/(mK) to ~3500 W/(mK). Both these values are 4 orders of magnitude higher than the thermal conductivity of the matrix material used herein (see Table 1). We take advantage of this difference in our computational algorithm, by distributing the heat markers uniformly inside a SWNT (see the rules of marker motion below). Using the effective medium theory,[21] one can determine[12] that the effects of the aspect ratio on the effective thermal conductivity are negligible for $L/D > 20$, when there is no percolation through the composite and when the aspect ratio is large, but not infinite. (Note that, according to the effective medium theory analysis of Nan et al.[21] for the case of composites with inclusions that exhibit thermal resistance at the interface between the inclusions and the matrix material, when L is comparable or equal to the dimensions of the composite, the effective thermal conductivity of the medium for long continuous fibers becomes equal to the result found by the rule of mixtures.[21]) In the simulations conducted in this study, an aspect ratio of $L/D = 40$, 80, and 120 was chosen, and the SWNT diameter was set to be constant with a value of $D = 2.40$ nm.[12]

The computation of the effective transport coefficients is based on an off-lattice Monte Carlo that has been described at length elsewhere.[12,15] The computational domain for the numerical simulation is a rectangular cell with SWNTs dispersed randomly and with random orientation. Because the SWNTs are not allowed to be in contact with each other (see rule 2 below), a new randomly oriented SWNT is generated by the algorithm in place of any SWNT that is found to be in contact with other SWNTs in the domain. The size of the computational domain for the simulations is presented in Table 2. The computational cell is heated from one surface (the $x = 0$ plane) with the release of 90 000 walkers distributed randomly and uniformly on that surface. The walkers exit at the surface opposite to the heated surface. The cell is periodic in the other two directions. The displacement of the walkers in the matrix is due to Brownian motion and can be described by a normal distribution with a zero mean and a standard deviation that depends on the matrix thermal diffusivity, D_m. The standard deviation of the distribution in each one of the space dimensions is $\sigma = \sqrt{2D_m\Delta t}$, where Δt is the time increment. The Brownian motion trajectories of all of these random walkers are monitored in time and space until steady state occurs, which in this case is for 100 ns, with a time increment of 0.02 ns. The temperature distribution is calculated from the number of walkers found in each bin of the computational domain, and it is proportional to the number of walkers in each bin.[15]

The details of the algorithm and the physical assumptions of our approach are detailed in ref 12. In summary, the rules of motion of the random walkers are (1) walkers distribute uniformly once inside the SWNTs due to the high SWNT thermal conductivity relative to the thermal conductivity of the surrounding material; (2) the SWNTs are assumed to be dispersed in a way that they do not form bundles (i.e., no SWNT−SWNT contact) and are not bent; (3) the transfer of heat is passive; (4) the thermal boundary resistance is the same for walkers coming in and out the SWNTs and is the same for the cylindrical wall and for the ends of the SWNTs; that is, once a walker in the fluid reaches the interface between the fluid and a SWNT, the walker will move into the SWNT phase with a probability $f_{\text{f-CN}}$, which represents the thermal resistance of the interface and will stay at the previous position in the fluid with a probability of $1 - f_{\text{f-CN}}$. Similarly, once a walker is inside a SWNT, the walker will redistribute randomly within the SWNT with a probability of $1 - f_{\text{CN-f}}$ at the end of a time step, and will cross into the fluid phase with a probability $f_{\text{CN-f}}$; (5) the volume fraction of SWNTs in every slice (i.e., every x plane) of the computational domain is equal to the volume fraction of the SWNTs in the composite, so that the weighted average of the product of the density times the heat capacity for a slice of the composite is the same throughout the domain; and (6) the boundaries on the y and z sides are treated as periodic, while those in the x (perpendicular to the applied flux) are treated as hard walls (i.e., the walkers bounce back when colliding with these walls).

3. Results and Discussion

3.1. Effects of Aspect Ratio, Weight Fraction of SWNTs, and Thermal Boundary Resistance on the Thermal Conductivity of SWNT−Water and SWNT−Oil Suspensions.

TABLE 2: Summary of the Simulation Parameters and Simulation Results of the SWNT Dispersed Randomly in the Suspensions

simulation parameters		computational cell: 100 × 100 × 100 nm^3 (L/D = 40) 200 × 100 × 100 nm^3 (L/D = 80) 300 × 100 × 100 nm^3 (L/D = 120) number of walkers: 90 000 SWNT diameter: 2.4 nm thermal equilibrium value C_f: 0.25 time increment: 0.002 ns ratios of L/D: 40−120								
$f_{\text{fluid-CN}}$	R_{bd} [10^{-8} m^2·K/W] (K_{bd}, [MW/m^2·K])	Weight Fractions of SWNTs, wt %								
		0.5	1.0	2.0	0.5	1.0	2.0	0.5	1.0	2.0
		L/D = 40	40	40	L/D = 80	80	80	L/D = 120	120	120
		$K_{\text{eff}}/K_{\text{water}}$, SWNTs Dispersed Randomly in Water at 20 °C								
volume fraction, vol % (number of SWNTs):		9 (214)	17 (393)	29 (678)	9 (214)	17 (393)	29 (678)	9 (214)	17 (393)	29 (678)
0.003[a]	20.000 (5)	0.95	0.95	0.96	1.40	1.59	1.77	1.56	1.79	2.01
0.008[b]	8.310 (12)	1.06	1.13	1.21	1.82	2.12	2.41	2.03	2.36	2.67
0.100	0.640 (156)	2.20	2.73	3.22	4.24	5.07	5.91	4.38	5.26	6.14
1.000	0.064 (1563)	4.01	5.25	6.44	7.20	8.98	10.08	7.31	9.09	11.04
		$K_{\text{eff}}/K_{\text{oil}}$, SWNTs Dispersed Randomly in Oil at 40 °C								
volume fraction, vol % (number of SWNTs):		7 (178)	14 (333)	25 (587)	7 (178)	14 (333)	25 (587)	7 (178)	14 (333)	25 (587)
0.037[c]	4.000 (25)	1.59	2.14	3.70	2.65	3.19	3.73	2.89	3.45	4.01
0.100	1.488 (67)	1.88	2.64	4.78	3.51	4.26	5.03	3.73	4.48	5.30
1.000	0.149 (671)	2.24	3.21	6.02	5.67	7.09	8.68	5.68	7.15	8.78

[a] Calculated from the thermal boundary resistance obtained from the MD work of Maruyama et al.[10] [b] Calculated from the thermal boundary resistance obtained from experimental work of Huxtable et al.[11] [c] Calculated from the thermal boundary resistance obtained from the MD simulation of Octane of Huxtable et al.[11]

The suspensions used for the simulations were water at 20 °C and oil at 40 °C. The SWNTs were randomly oriented, and the location of the SWNTs was random. The number of SWNTs in the cubic computational cell varied from 214 to 678 for the SWNT−water suspension at 20 °C, and from 178 to 587 for the SWNT−oil at 40 °C, and depended on the weight fraction of SWNTs in the suspensions. The thermal boundary resistance was chosen on the basis of the experimental and MD simulation studies of Huxtable et al.[11] and Maruyama et al.[10] that have provided estimations of the thermal boundary resistance in conditions similar to the simulations. According to the acoustic theory for the interpretation of thermal resistance,[8] the average probability for transmission of phonons across the interface into the carbon nanotube, $f_{\text{f-CN}}$, is related to the thermal boundary resistance, R_{bd}, by

$$f_{\text{f-CN}} = \frac{4}{\rho C C_m R_{bd}} \quad (1)$$

where ρ is the fluid density; C is the fluid specific heat; and C_m is the velocity of sound in the surrounding fluid. The simulations were conducted with different weight fractions of SWNTs (0.5%, 1.0%, and 2.0%) and with different thermal boundary resistance ($f_{\text{f-CN}}$ = 1.000, 0.100, 0.003, 0.008 for water and $f_{\text{f-CN}}$ = 1.000, 0.100, 0.037 for oil).

The simulation parameters are presented in Table 2, as well as the ratios of the effective thermal conductivity and pure suspension thermal conductivity of the SWNT−oil at 40 °C and SWNT−water suspensions at 20 °C obtained from the simulation runs. The effective thermal conductivity is a function of the thermal boundary resistance, the SWNT weight fraction, and the length scale of SWNTs in the suspensions. For each value of thermal boundary resistance, weight fraction, and aspect ratio of SWNTs, the reported thermal conductivity is the average of three separate simulations with different initial SWNT distributions. The standard deviation of the simulation results was within 0.5% of the average value. With the same thermal boundary resistance and the same aspect ratio L/D, the effective thermal conductivities of both SWNT suspensions increase when the weight fraction of SWNTs increases. When the thermal boundary resistance decreases, heat can be transferred easier through the fluid−SWNT interface into the SWNTs, and then transferred through the suspension quite effectively, because the SWNTs have high thermal conductivity. So the effective thermal conductivities of both SWNT suspensions increase, as expected. When the thermal boundary resistance is very large, as in the SWNT−water suspension case, the thermal walkers cannot diffuse easily in the suspension because SWNT−fluid interface resists walkers entering the SWNTs, effectively blocking the diffusion of heat through the suspension. When diffusion is blocked by the SWNTs, the effective thermal conductivity of the SWNT suspension can be decreased, and even become smaller than that of the pure suspension fluid.

Figure 1 presents the simulation results for the ratio of the effective thermal conductivity of the suspensions divided by the thermal conductivity of water and pure oil at 20 °C as a function of the thermal boundary resistance and with different aspect ratios of SWNTs (L/D = 40−120) in the suspensions having 1.0 wt % of the SWNTs. Figure 1 shows that the thermal conductivity of the SWNT suspensions increases between the case of L/D = 40 and the case of L/D = 80, but becomes almost constant when the aspect ratio L/D is greater than 80. At the lowest thermal boundary resistance for both suspensions ($f_{\text{f-CN}}$ = 1.0), the difference of the thermal conductivity enhancement of the SWNT−water and −oil suspensions with the aspect ratios L/D = 80 and 120 is approximately 1%. This means that once the aspect ratio is large enough, the thermal conductivity of the

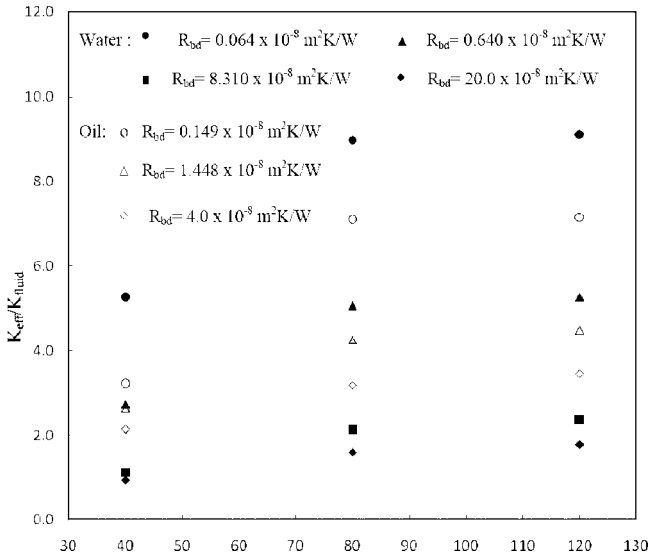

Figure 1. Length scale effect on the effective thermal conductivity of SWNT−water and −oil suspensions with 1.0 wt % of the SWNTs. For each value of thermal boundary resistance and aspect ratio of SWNTs, the thermal conductivity is the average of three simulations with different initial SWNT distributions.

SWNT suspensions is independent of *L*/*D*. This trend of the simulation results agrees qualitatively with the analytical solution of Nan et al.[21] that indicates *L*/*D* independence for large *L*/*D*.

The effective thermal conductivity using thermal boundary resistance up to 0.4 × 10^{-7} m^2·K/W (K_{bd} = 25 MW/m^2·K) at *L*/*D* = 40 and at *L*/*D* =120, respectively, is shown on Figure 2a and b. Because the effective thermal conductivities decrease dramatically with increasing thermal boundary resistance in Figure 2, it is essential to choose the proper thermal boundary resistance within the range of (0.4−2.0) × 10^{-7} m^2·K/W (K_{bd} = 5−25 MW/m^2·K) for validation with experimental data, when they might become available. At the thermal boundary resistance of 0.83 × 10^{-7} m^2·K/W (K_{bd} = 12 MW/m^2·K), the effective thermal conductivity of the SWNT−water suspensions can be enhanced only up to 20% at 2.0 wt % of SWNTs for short nanotubes (*L*/*D* = 40), but up to 167% for long nanotubes. At the lowest thermal boundary resistance simulated for the oil case (R_{bd} = 0.1488 × 10^{-8} m^2·K/W), the effective thermal conductivity of the SWNT−oil suspension can be enhanced 5.9, 7.2, and 8.8 times with 0.5%, 1.0%, and 2.0 wt % of SWNTs in the oil, respectively, for long nanotubes (see Figure 2b). At the lowest thermal boundary resistance simulated for the water case (R_{bd} = 0.064 × 10^{-8} m^2·K/W), the effective thermal conductivity of the SWNT−water suspension at 20 °C can be enhanced 7.3, 9.1, and 11.0 times with 0.5%, 1.0%, and 2.0 wt % of SWNTs in the water, respectively, for long nanotubes.

It is also seen in Figure 2 that, with the same thermal boundary resistance, the SWNT weight fraction is more important in the oil suspension case. Because the specific heat capacity of oil is one-half of that of water (the values of other physical properties are almost the same), the value of $f_{f\text{-}CN}$ for oil calculated by eq 2 is 2 times higher than that for SWNT−water. (The specific heat capacities of oil and water are 2.22 and 4.18 J/g·K, respectively.) This means that phonons can cross the interface of oil and SWNTs more easily than the interface of water and SWNTs. It appears, therefore, that fluids with larger molecules can be more effective in transferring heat to SWNTs suspended in them.

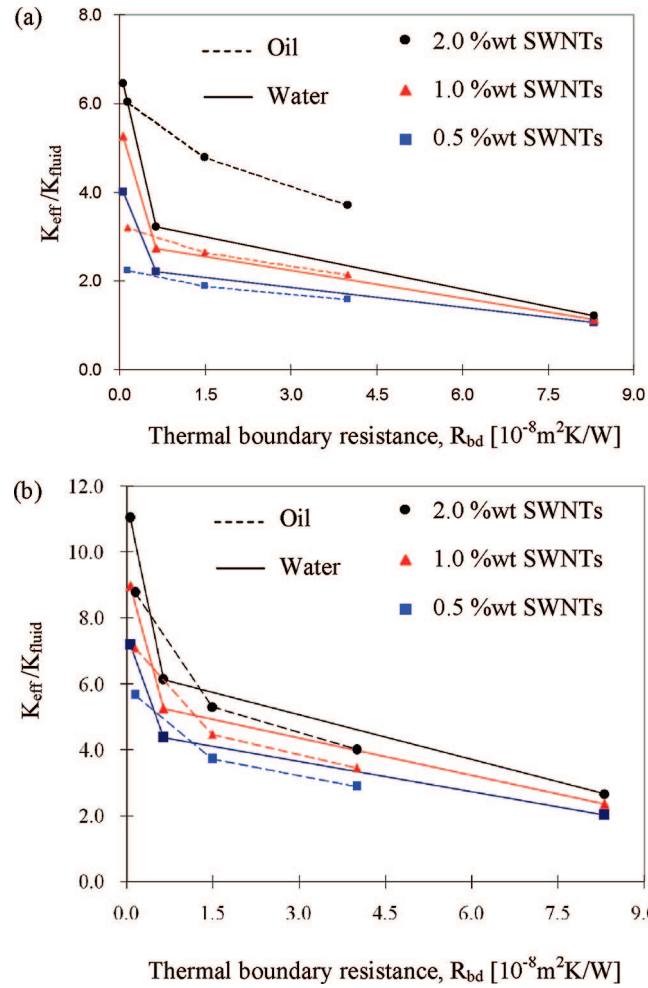

Figure 2. Effective thermal conductivity of randomly dispersed SWNT−oil and SWNT−water suspension at (a) *L*/*D* = 40 and (b) *L*/*D* = 120. For each value of thermal boundary resistance and weight fraction of SWNTs, the thermal conductivity is the average of three simulations with different initial SWNT distributions.

3.2. Temperature Effects on the Thermal Conductivity of the SWNT−Water Suspensions. The simulations to study the effect of the suspension temperature on the effective thermal conductivity of the SWNT−water suspensions were conducted similarly to the water case at 20 °C, described in section 3.1. The aspect ratio *L*/*D* = 120 is used. Each of the simulations was conducted assuming that the properties of SWNTs and water were constant for the temperature interval employed in that particular simulation. This is equivalent to applying a very small temperature difference (e.g., less than 1 °C) across the computational domain in each simulation, and repeating this process at different temperatures.

The simulations were conducted at different temperatures (20, 40, 60, and 80 °C), with different weight fractions of SWNTs (0.5%, 1.0%, and 2.0%). The SWNTs were randomly oriented, and the location of the SWNTs was random. The number of SWNTs in the cubic cell varied from 214 to 678.

Because currently available data for the thermal boundary resistance of SWNTs in fluids indicate a range of values between 0.83 × 10^{-7} m^2·K/W (K_{bd} = 12 MW/m^2·K)[11] and 2 × 10^{-7} m^2·K/W (K_{bd} = 5 MW/m^2·K),[10] simulations were conducted using specifically these two values. It was further assumed that the thermal boundary resistance has a constant value in the temperature range studied here. This assumption is justified because the ratio of the thermal diffusivity of the SWNTs

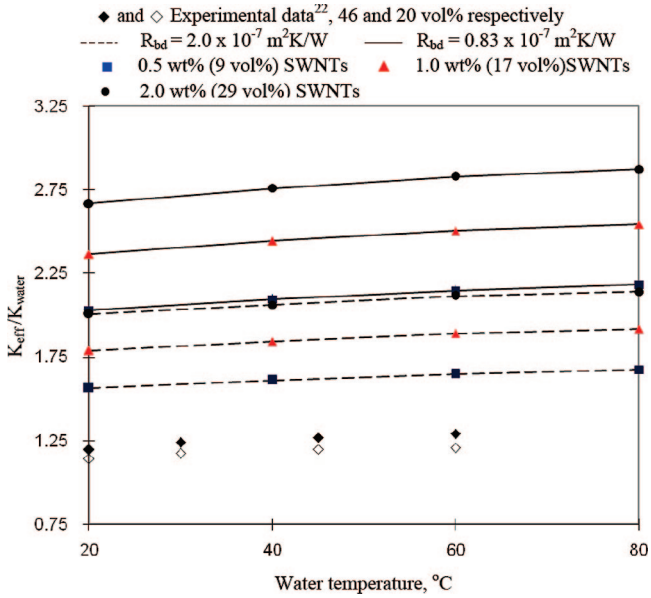

Figure 3. Temperature effect on the effective thermal conductivity of SWNT−water suspension at L/D =120. For each value of thermal boundary resistance and weight fraction of SWNTs, the thermal conductivity is the average of three simulations with different initial SWNT distributions. The experimental data are for MWNT suspensions.[22]

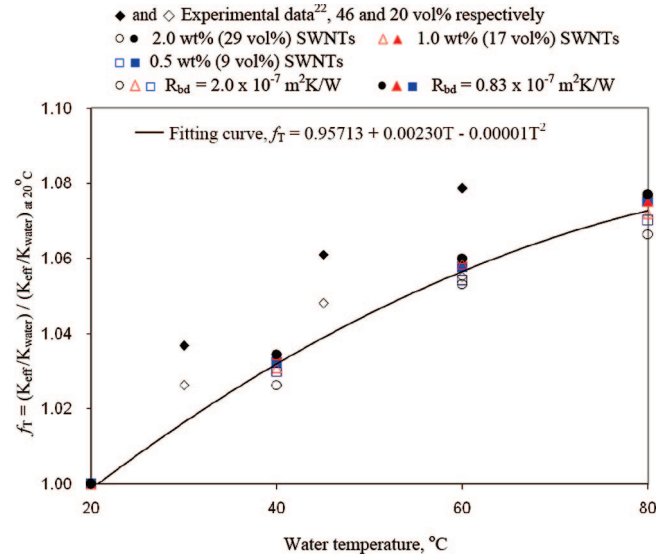

Figure 4. Temperature effect on the ratio of K_{eff}/K_{water} divided by K_{eff}/K_{water} at 20 °C. The experimental data are for MWNT suspensions.[22]

divided by the thermal diffusivity of the water at each one of the temperatures studied differs by less than 5% (the thermal diffusivity of water at different temperatures is listed in Table 1, and the thermal diffusivity of SWNTs remains constant in this temperature interval). In addition, the product of the specific heat capacity times density of water at different temperatures, which is a term appearing in the equation that is used to calculate the thermal boundary resistance (eq 2), decreases less than 2.5% in the temperature range examined. The velocity of sound in water is also constant in this temperature regime. Because the thermal boundary resistance is affected by these factors, one can reasonably assume that it will vary by less than 5%, and one can model the value of the thermal boundary in the simulations as a constant. By applying eq 1 with constant R_{bd} and using the properties of water from Table 1, the value of $f_{w\text{-}CN}$ increases slightly with temperature.

The physical properties of water at different temperatures are summarized in Table 1. Figure 3 shows the temperature effect on the effective thermal conductivity of SWNT−water suspension. The reported thermal conductivity is the average of three simulation runs with different initial SWNT random distributions. With the same weight fraction of SWNTs and the same thermal boundary resistance, the effective thermal conductivities of the SWNT−water suspension increase when the temperature increases, due to enhanced diffusion of the heat walkers. This result is consistent with experimental measurements of previous researchers for multiwalled carbon nanotube nanofluids[22,23] (as shown in Figure 3) and for carbon nanotube/epoxy.[3] Once the weight fraction of SWNTs increases, the effective thermal conductivity increases under the same suspension temperature and the same thermal boundary resistance. When the temperature of water increases from 20 to 80 °C, the thermal conductivity of the suspension can be enhanced by up to 8%.

A temperature enhancement factor f_T can be defined as the ratio of K_{eff}/K_{water} divided by K_{eff}/K_{water} at 20 °C. This factor is shown in Figure 4 as a function of temperature. Under the same water temperature, the factor f_T is almost constant and independent of the weight fraction of SWNTs in the water and of the thermal boundary resistance. By fitting the calculated f_T data, we can obtain the following equation:

$$f_T = 0.95713 + 0.00230T - 0.00001T^2 \qquad (2)$$

where T is the water temperature (in °C) and the coefficient R^2 for the fit is 0.98. Figure 4 also shows data points obtained from the experiments of multiwalled carbon nanotubes (MWNTs) in suspension reported by Wen and Yulong.[22] (Note that the surfactant used in the work of Wen and Yulong to suspend the MWNTs was similar to the surfactant used in the work of Huxtable et al.[11]) The experimental data fall above the empirical fit suggested by eq 2 for 46% vol MWNT and closer to the fit for 20% vol. The enhancement factor f_T does not increase dramatically, but, nevertheless, eq 2 is independent of the weight fraction of the SWNTs and the thermal boundary resistance. Therefore, this equation can predict the increase of the ratio K_{eff}/K_{water} with the water temperature. Because the equation has been obtained empirically, one should be careful not to extend outside its range of applicability for cases outside the range of SWNT weight fractions used here.

4. Conclusions

A computational model for systematically studying the effects of the thermal boundary resistance, weight fraction, and the aspect ratio of SWNTs in oil and in water, as well as the effect of different water temperature on the thermal conductivity of SWNT−water suspensions, using a random walk algorithm has been successfully developed. This model can be applied to any suspension with a very wide range of weight fraction of SWNTs in the suspension, given that the inclusions are not in contact with each other.

In both SWNT−oil and SWNT−water suspensions, the effective thermal conductivity increases once the weight fraction of the SWNTs increases and the thermal boundary resistance is kept constant. With the same SWNT weight fraction, the effective thermal conductivity increases when the thermal boundary resistance decreases. The simulation results indicate that fluids with larger molecules can be more effective in transferring heat to SWNTs suspended in them. Increasing the suspension temperature can enhance the thermal conductivity

of the SWNT−water systems, and this enhancement can be described as a function of temperature only, independent of weight fraction and thermal boundary resistance.

Acknowledgment. This work was supported by the National Computational Science Alliance under CTS-040023 and by the TeraGrid under TG-CTS070037T, and it utilized the NCSA IBMp690.

References and Notes

(1) Ajayan, P. M.; Schadler, L. S.; Giannaris, C.; Rubio, A. Single-walled carbon nanotube-polymer composites: Strength and weakness. *Adv. Mater.* **2000**, *12*, 750.

(2) Choi, S. U. S.; Zhang, Z. G.; Yu, W.; Lockwood, F. E.; Grulke, E. A. Anomalous thermal conductivity enhancement in nanotube suspensions. *Appl. Phys. Lett.* **2001**, *79*, 2252–2254.

(3) Biercuk, M. J.; Llaguno, M. C.; Radosavljevic, M.; Hyun, J. K.; Johnson, A. T.; Fischer, J. E. Carbon nanotube composites for thermal management. *Appl. Phys. Lett.* **2002**, *80*, 2767–2769.

(4) Maxwell, J. C. *A Treatise on Electricity and Magnetism*, 2nd ed.; Clarendon Press: Oxford, UK, 1881.

(5) Hamilton, R. L.; Crosser, O. K. Thermal conductivity of heterogeneous 2-component systems. *I&EC Fundam.* **1962**, *1*, 187.

(6) Keblinski, P.; Phillpot, S. R.; Choi, S. U. S.; Eastman, J. A. Mechanisms of heat flow in suspensions of nano-sized particles (nanofluids). *Int. J. Heat Mass Transfer* **2002**, *45*, 855–863.

(7) Kapitza, P. L. *J. Phys. Moscow* **1941**, *4*, 181.

(8) Swartz, E. T.; Pohl, R. O. Thermal-boundary resistance. *Rev. Mod. Phys.* **1989**, *61*, 605–668.

(9) Maruyama, S.; Kimura, T. A study on thermal resistance over a solid-liquid interface by the Molecular Dynamics method. *Therm. Sci. Eng.* **1999**, *7*, 63–68.

(10) Maruyama, S.; Igarashi, Y.; Taniguchi, Y.; Shiomi, J. Anisotropic heat transfer of single-walled carbon nanotubes. *J. Therm. Sci. Technol.* **2006**, *1*, 138–148.

(11) Huxtable, S. T.; Cahill, D. G.; Shenogin, S.; Xue, L.; Ozisik, R.; Barone, P.; Usrey, M.; Strano, M. S.; Siddons, G.; Shim, M.; Keblinski, P. Interfacial heat flow in carbon nanotube suspensions. *Nat. Mater.* **2003**, *2*, 731–734.

(12) Duong, M. H.; Papavassiliou, D. V.; Mullen, J. K.; Maruyama, S. Computational modeling of thermal conductivity of single walled carbon nanotube polymer composites. *Nanotechnology* **2008**, *19*, 065702.

(13) Tomadakis, M. M.; Sotirchos, S. V. Transport-properties of random arrays of freely overlapping cylinders with various orientation distributions. *J. Chem. Phys.* **1993**, *98*, 616–626.

(14) Tomadakis, M. M.; Sotirchos, S. V. Transport through random arrays of conductive cylinders dispersed in a conductive matrix. *J. Chem. Phys.* **1996**, *104*, 6893–6900.

(15) Duong, M. H.; Papavassiliou, D. V.; Mullen, J. K.; Lee, L. L. Random walks in nanotube composites: Improved algorithms and the role of thermal boundary resistance. *Appl. Phys. Lett.* **2005**, *87*, 013101.

(16) Garcia, E. J.; Wardle, B. L.; Hart, A. J.; Yamamoto, N. Fabrication and multifunctional properties of a hybrid laminate with aligned carbon nanotubes grown in situ. *Compos. Sci. Technol.* **2008**, *68*, 2034–2041.

(17) Garcia, E. J.; Wardle, B. L.; Hart, A. J. Joining prepreg composite interfaces with aligned carbon nanotubes. *Composites Part A* **2008**, *39*, 1065–1070.

(18) Murakami, Y.; Einarsson, E.; Edamura, T.; Maruyama, S. T. Polarization dependent optical absorption properties of single-walled carbon nanotubes and methodology for the evaluation of their morphology. *Carbon* **2005**, *13*, 2664–2676.

(19) Maruyama, S. A Molecular Dynamics Simulation of Heat Conduction of Finite Length SWNTs. *Physica B*, **2002,** *323*, 193–195.

(20) Wang, Z. L.; Tang, D. W.; Zheng, X. H.; Zhang, W. G.; Zhu, Y. T. Length-dependent thermal conductivity of single-wall carbon nanotubes: prediction and measurements. *Nanotechnology* **2007**, *18*, 475714.

(21) Nan, C. W.; Birringer, R.; Clarke, D. R.; Gleiter, H. Effective thermal conductivity of particulate composites with interfacial thermal resistance. *J. Appl. Phys.* **1997**, *81*, 6692–6699.

(22) Wen, D.; Yulong, D. Efective thermal conductivity of aqueous suspensions of carbon nanotubes (Carbon nanotube nanofluids). *J. Therm. Heat Transfer* **2004**, *18*, 481–485.

(23) Das, S. K.; Putra, N.; Thiesen, P.; Roetzal, W. Temperature dependence of thermal conductivity enhancement for nanofluids. *J. Heat Transfer−ASME Trans.* **2003**, *125*, 567–574.

(24) Glavatskih, S. B.; Fillon, M.; Larsson, R. The significance of oil thermal properties on the performance of a tilting-pad thrust bearing. *J. Tribology - ASME Trans.* **2002**, *124*, 377–385.

(25) Lide, D. R. *CRC Handbook of Chemistry and Physics*, 72nd ed.; CRC Press Inc.: Ann Arbor/Boston, 1991; Vols. *6*−*9*, pp 6−10.

(26) Lide, D. R. *CRC Handbook of Chemistry and Physics: Velocity of Sound in Various Media*, 72nd ed.; CRC Press Inc.: Ann Arbor/Boston, 1991; pp 14−35.

JP710021N